

LETTER TO THE EDITOR

Strong [CII] emission at high redshift^{★,★★}

R. Maiolino¹, P. Caselli², T. Nagao³, M. Walmsley⁴, C. De Breuck⁵, and M. Meneghetti^{6,7}

¹ INAF – Osservatorio Astronomico di Roma, via di Frascati 33, 00040 Monte Porzio Catone, Italy
e-mail: maiolino@oa-roma.inaf.it

² School of Physics and Astronomy, University of Leeds, Leeds LS2 9JT, UK

³ Research Center for Space and Cosmic Evolution, Ehime University, 2-5 Bunkyo-cho, Matsuyama 790-8577, Japan

⁴ Osservatorio Astrofisico di Arcetri, Largo E. Fermi 5, 50125 Firenze, Italy

⁵ European Southern Observatory, Karl Schwarzschild Strasse 2, 85748 Garching, Germany

⁶ INAF – Osservatorio Astronomico di Bologna, via Ranzani 1, 40127 Bologna, Italy

⁷ INFN, Sezione di Bologna, viale Berti Pichat 6/2, 40127 Bologna, Italy

Received 3 April 2009 / Accepted 21 April 2009

ABSTRACT

We report the detection of the [CII]157.74 μm fine-structure line in the lensed galaxy BRI 0952-0115 at $z = 4.43$, using the APEX telescope. This is the first detection of the [CII] line in a source with $L_{\text{FIR}} < 10^{13} L_{\odot}$ at high redshift. The line is much stronger than previous [CII] detections at high- z (a factor of 5–8 higher in flux), partly due to the lensing amplification. The $L_{[\text{CII}]} / L_{\text{FIR}}$ ratio is $10^{-2.9}$, which is higher than observed in local galaxies with similar infrared luminosities. Together with previous observations of [CII] at high redshift, our result suggests that the [CII] emission in high-redshift galaxies is enhanced relative to local galaxies with the same infrared luminosity. This finding may result from selection effects of the few current observations of [CII] at high redshift and, in particular, from non detections that may not have been published (although the few published upper limits are still consistent with the [CII] enhancement scenario). If the trend is confirmed with larger samples, it would indicate that high- z galaxies are characterized by different physical conditions than for their local counterparts. Regardless of the physical origin of the trend, this effect would increase the potential of the [CII]158 μm line to search and characterize high- z sources.

Key words. galaxies: high-redshift – galaxies: ISM – submillimeter – infrared: galaxies

1. Introduction

The $^2\text{P}_{3/2} \rightarrow ^2\text{P}_{1/2}$ fine-structure line of C^+ at 157.74 μm is emitted primarily by gas exposed to ultraviolet radiation in the photo dissociation regions (PDRs) associated with star-forming activity (even in galaxies hosting AGNs). This line is generally the brightest emission line in the spectrum of galaxies, accounting for as much as ~ 0.1 – 1% of their total luminosity (Crawford et al. 1985; Stacey et al. 1991; Wright et al. 1991). As a consequence, the [CII]158 μm line is regarded as the most promising tool for detecting and identifying high-redshift galaxies with forthcoming (sub-)mm facilities, such as ALMA (e.g. Maiolino 2008).

In local galaxies, with far-infrared luminosities $L_{\text{FIR}} < 10^{11} L_{\odot}$, the [CII] luminosity is proportional to the far-IR luminosity and typically $-3 \leq \log(L_{[\text{CII}]} / L_{\text{FIR}}) \leq -2$ (e.g. Stacey et al. 1991). However, for sources with $L_{\text{FIR}} > 10^{11}$ – $10^{11.5} L_{\odot}$, this ratio drops by an order of magnitude (Malhotra et al. 2001; Luhman et al. 1998, 2003; Negishi et al. 2001). Various explanations have been proposed for the physical origin of this effect, more specifically: 1) a high ratio of ultraviolet flux to gas density, which results in positively charged dust grains that in turn reduce the efficiency of the gas heating by the photoelectric effect (e.g. Kaufman et al. 1999), and which also increases the fraction of

UV radiation absorbed by dust (Abel et al. 2009); 2) opacity effects that weaken the [CII] emission line in infrared luminous galaxies (Gerin & Phillips 2000; Luhman et al. 1998); 3) contribution to L_{FIR} from dust associated with HII regions (Luhman et al. 2003); 4) contribution to L_{FIR} from an AGN (see Malhotra et al. 2001). Regardless of the physical origin of the effect, the sharp drop in the $L_{[\text{CII}]} / L_{\text{FIR}}$ ratio at high luminosities has cast doubts about the usefulness on the [CII] to trace high- z galaxies.

Although locally the [CII]158 μm line can only be observed from space or from airborne observatories, at high redshift the line is shifted into the submm-mm windows of atmospheric transmission, so that it can be observed with groundbased facilities. The first detection of the [CII]158 μm was obtained in J114816.64+525150.3, one of the most distant quasars known at $z = 6.4$, for which the [CII] line is shifted at 1.2 mm (Maiolino et al. 2005; Walter et al. 2009). The second most distant [CII] detection was obtained in BR 1202–0725, a quasar at $z = 4.7$ (Iono et al. 2006). Both these sources have luminosities $L_{\text{FIR}} > 10^{13} L_{\odot}$ (Hyper Luminous Infrared Galaxies, HyLIRGs)¹, and actually these are the first [CII] detections in galaxies with such high

¹ Note that the “standard definition” of LIRG, ULIRG, and HyLIRG is based on the total infrared luminosity ($L_{\text{IR}} = L(8\text{--}1000) \mu\text{m}$), and specifically the three classes are defined with $L_{\text{IR}} > 10^{11}$, $> 10^{12}$, $> 10^{13} L_{\odot}$, respectively (Sanders & Mirabel 1996). Throughout the paper we instead use the far-IR luminosity, defined as $L_{\text{FIR}} = L(40\text{--}500) \mu\text{m}$, which is generally more accurately constrained and reported for high- z sources and which can be lower than L_{IR} by a factor ranging from 1.1 to 2 depending on the source.

[★] Based on observations made with ESO telescope APEX, under program ID E-082.B-0692A-2008.

^{★★} Appendix A is only available in electronic form at <http://www.aanda.org>

luminosities. In these objects $\log(L_{[\text{CII}]} / L_{\text{FIR}}) \approx -3.5$, i.e. similar to the value observed in local Ultra-Luminous Infrared Galaxies (ULIRGs) with luminosities $10^{12} < L_{\text{FIR}} < 10^{13} L_{\odot}$. This result is somewhat surprising, since the extrapolation of the rapidly decreasing $L_{[\text{CII}]} / L_{\text{FIR}}$ observed in local ULIRGs would predict a much lower [CII] luminosity than observed in the two extremely luminous objects at high- z detected so far. Possibly, evolutionary effects are involved.

To further investigate the latter issue one should search for [CII] emission in high- z galaxies with infrared luminosity closer to the local ULIRGs for which [CII] has been observed, i.e. $L_{\text{FIR}} \approx 10^{12} - 10^{12.5} L_{\odot}$. The quasar BRI 0952-0115 at $z = 4.4337$ is an optimal source for this test. This is a lensed quasar with a magnification factor in the range $\mu = 2.5 - 8$ (see Appendix), whose mm and submm fluxes (fitted with a modified black body) indicate an intrinsic (de-magnified) far-IR luminosity $L_{\text{FIR}} \sim 4 \times 10^{12} L_{\odot}$ (Priddey & McMahon 2001, corrected for our adopted cosmology). This quasar has also been detected in the molecular transition CO(5–4) (Guilloteau et al. 1999) that accurately determines its redshift, which is required for searching the [CII] within the narrow band offered by current submm receivers. We used the Atacama Path Finder Experiment (APEX)² to observe the [CII] line in BRI 0952-0115. In this letter we report the successful detection of the line. We discuss some possible implications of our detection on the physics of high-redshift galaxies and on the detectability of the [CII] line in general in high-redshift sources. We assume the concordance Λ -cosmology with $H_0 = 71 \text{ km s}^{-1} \text{ Mpc}^{-1}$, $\Omega_{\Lambda} = 0.73$, and $\Omega_{\text{m}} = 0.27$ (Spergel et al. 2003).

2. Observations and results

BRI 0952-0115 (RA(J2000) = 09:55:00.1, Dec(J2000) = -01:30:07.1) was observed with the Swedish Heterodyne Facility Instrument (SHFI, Vassilev et al. 2008) on the APEX telescope in six observing runs, from November 1 to December 18, 2008 (a short run on October 23 was totally discarded because of bad weather conditions), for a total of about 22 h of observations, including sky observations and overheads, resulting in 5 h of net on-source integration. The weather conditions were generally very good with precipitable water vapor $0.25 < p_{\text{wv}} < 1.0 \text{ mm}$, the best-quality data coming from the run on December 17 when we had $p_{\text{wv}} < 0.5 \text{ mm}$ for 6 h. We used the APEX-2 receivers tuned to 349.77 GHz (both polarizations), which is the expected frequency of the [CII]157.741 μm line at the redshift $z = 4.4337$ provided by the CO(5–4) detection (Guilloteau et al. 1999). At this frequency the 1 GHz band of the back-end translates into a velocity coverage of about 860 km s^{-1} . In the last run (December 18) we also observed with the frequency of the two receivers offset by $\pm 200 \text{ km s}^{-1}$, to check the effects of possible instrumental artifacts. Observations were done in wobbler-switching mode, with a symmetrical azimuthal throw of $20''$ and a frequency of 0.5 Hz. Pointing was checked on the nearby source IRC+10216 every 1–2 h and found to be better than $3''$ (with a beam size of $18''$). The focus was checked on Saturn, especially after sunrise when the telescope deformations are largest.

The data were analyzed by using CLASS (within the GILDAS-IRAM package). One of the main problems in searching for relatively broad lines (a few hundred km s^{-1}) with

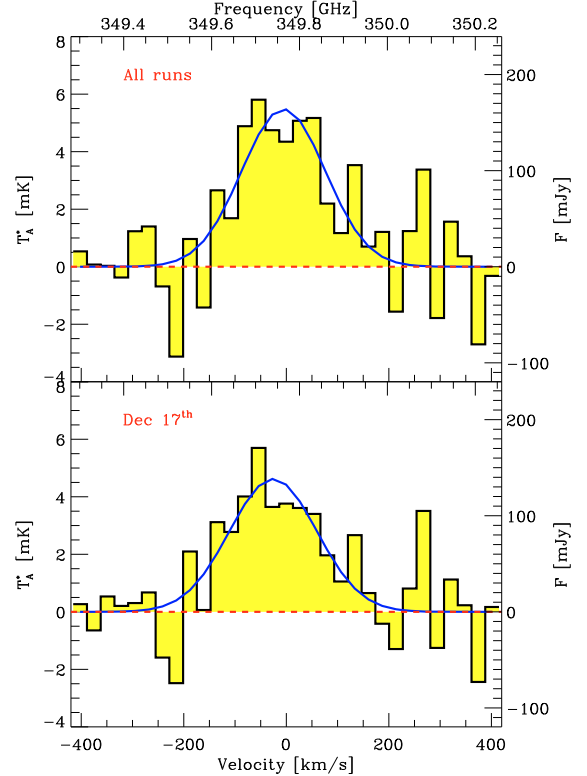


Fig. 1. Spectrum of the [CII] 157.74 μm emission line in the quasar BRI 0952-0115 at $z = 4.4337$ shown with a velocity resolution of 27 km s^{-1} (see text for details). The blue curve shows the Gaussian fit to the line profiles (see Table 1).

single-dish telescopes are the spectral baseline instabilities. As a consequence, we visually inspected all individual scans and removed those with clear baseline instabilities. We found that the analysis further benefits from additional purging of scans that show a rms higher than a given threshold. This technique removes additional baseline instabilities that are not readily seen in the visual inspection of individual scans. The lower the rms threshold, the lower the “noise” introduced by spurious baselines, but an increasing fraction of scans is discarded causing the Poisson noise to increase. We found that an rms threshold of 130 mK optimizes the noise in the spectra (which leaves about 1.6 h of on-source integration), although the results do not change significantly as long as the rms threshold is below about 145 mK (which would include 60% of the observing time). To show that the final result does not depend significantly on the scan selection (as long as the really bad ones are removed), we have also separately combined all scans of the best run, on December 17, without any rms rejection. The individual scans were aligned in frequency and averaged together. A linear baseline was subtracted to the final spectrum by interpolating the channels in the velocity ranges $-400 < v < -200 \text{ km s}^{-1}$ and $200 < v < 400 \text{ km s}^{-1}$.

Figure 1 shows the resulting spectrum smoothed to a spectral resolution of 27 km s^{-1} . The top panel is for the combination of all runs with the threshold rms $< 130 \text{ mK}$, while the bottom panel shows the combination of the December 17 run only (the best-weather run), without any rms rejection. The [CII] line is clearly detected, with a significance of 7σ . We also verified that, if we split the observations in two halves, the line is detected independently in each of them with a significance higher than about 5σ .

² APEX is a collaboration between the Max-Planck-Institut für Radioastronomie, the European Southern Observatory, and the Onsala Space Observatory.

Table 1. Properties of the [CII] line observed toward BRI 0952-0115 compared with the CO(5–4) line observed by [Guilloteau et al. \(1999\)](#).

Line	ν_{rest} [GHz]	ν_{obs}	z_{line}	ΔV_{FWHM} [km s ⁻¹]	I [Jy km s ⁻¹]	$\log(L)^a$ [L_{\odot}]
[CII] ($^2P_{3/2}-^2P_{1/2}$)	1900.54	349.776	4.4336 ± 0.0003	193 ± 32	33.6 ± 4.9	9.66 ± 0.25
CO (5–4)	576.2679	106.055	4.4337 ± 0.0006	230 ± 30	0.91 ± 0.11	7.58 ± 0.25

^a Log of the luminosity corrected for a lensing magnification of $\mu = 4.5$, while the error reflects the possible range in magnifications $\mu = 2.5-8$ (see Appendix).

The [CII] line was fitted with a single Gaussian. The resulting line parameters are reported in Table 1, and compared with the CO(5–4) line detected by [Guilloteau et al. \(1999\)](#). The [CII] line center and width are fully consistent with those of the CO line.

3. Discussion

The previous two [CII]158 μm detections at high redshift ([Maiolino et al. 2005](#); [Iono et al. 2006](#)) were obtained in HyLIRGs ($L_{\text{FIR}} > 10^{13} L_{\odot}$). The observations presented in this paper toward BRI 0952-0115 provide the first [CII] detection at high redshift in a galaxy with luminosity $L_{\text{FIR}} < 10^{13} L_{\odot}$. A striking result is the strong line flux, 5–8 times higher than previous [CII] detections at high- z , with a peak intensity of 160 mJy. Such a strong flux is partly caused by the lensing amplification and partly by the lower luminosity distance with respect to previous [CII] detections.

The $L_{[\text{CII}]} / L_{\text{CO}(5-4)}$ ratio is about five times higher than inferred for the two other high- z sources with [CII] detection ([Maiolino et al. 2005](#); [Iono et al. 2006](#)). However, the last two sources are actually “CO-overluminous”, as shown by [Curran \(2009\)](#), and the observed difference is well within the spread between [CII] and CO luminosities observed in local LIRGs ([Curran 2009](#)). A direct comparison with local galaxies is not easy, since most of local galaxies have data for lower CO transitions, and the wide variations in the CO excitation, especially among high- z sources, makes it difficult to translate the CO(5–4) luminosity into a CO(1–0) luminosity (e.g. [Weiß et al. 2007](#)).

Probably the most important result of our observations is that the [CII] line in BRI 0952-0115 is very strong relative to its far-IR luminosity when compared to other luminous sources. This is illustrated in Fig. 2, which shows the $L_{[\text{CII}]} / L_{\text{FIR}}$ ratio versus L_{FIR} , both for local galaxies and high- z galaxies. We mark local galaxies for which the aperture used to measure [CII] (generally ISO-LWS) is smaller than 10 kpc, and therefore it may sample a smaller region relative to the beam (generally IRAS) used for the far-IR flux (hence the $L_{[\text{CII}]} / L_{\text{FIR}}$ ratio may not be reliable for some of these sources). Local galaxies show the well-known drop of the $L_{[\text{CII}]} / L_{\text{FIR}}$ ratio at luminosities $L_{\text{FIR}} > 10^{11} - 10^{11.5} L_{\odot}$. In BRI 0952-0115 we measure a ratio $\log(L_{[\text{CII}]} / L_{\text{FIR}}) = -2.93$ that is higher than observed in local ULIRGs, which are mostly in the range $-3.7 < \log(L_{[\text{CII}]} / L_{\text{FIR}}) < -3.2$. More interesting is the comparison of the trends of $L_{[\text{CII}]} / L_{\text{FIR}}$ in local and high- z galaxies. Figure 2 shows a linear fit (of the logarithmic quantities) to the local galaxies with $L_{\text{FIR}} > 10^{11} L_{\odot}$ (\sim LIRGs, see footnote 1), which describes the steep drop in $L_{[\text{CII}]} / L_{\text{FIR}}$ at high luminosities observed in local galaxies, in the form

$$\log\left(\frac{L_{[\text{CII}]}}{L_{\text{FIR}}}\right)_{\text{local}} = -1.43 \log(L_{\text{FIR},12}) - 3.47 \quad (1)$$

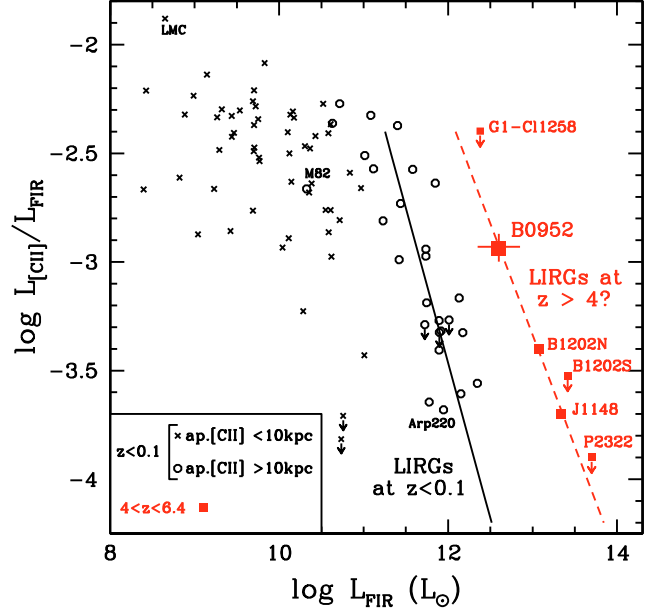


Fig. 2. $L_{[\text{CII}]} / L_{\text{FIR}}$ ratio versus L_{FIR} for normal and starburst local galaxies (black crosses and circles) and for high- z sources (red squares) (references are given in the text and in [Maiolino et al. 2005](#)). The [CII] detection reported here is marked with a red big symbol. The horizontal “errorbar” for BRI 0952-0115 reflects the possible range of lensing magnification factors (see Appendix). Black crosses indicate the galaxies for which the aperture to measure [CII] (ISO-LWS) is smaller than 10 kpc, and therefore it may sample a smaller region relative to the beam (IRAS) used for the far-IR flux. The black solid line shows a linear fit (of the logarithmic quantities) to the data of local luminous Infrared galaxies (LIRGs, $L_{\text{FIR}} > 10^{11} L_{\odot}$). The red dashed line is a linear fit to the detections at high redshift.

where $L_{\text{FIR},12}$ is the far-IR luminosity in units of $10^{12} L_{\odot}$. The extrapolation of the black line to high luminosities heavily underpredicts the $L_{[\text{CII}]} / L_{\text{FIR}}$ ratio observed in high- z sources. The high $L_{[\text{CII}]} / L_{\text{FIR}}$ ratio observed in BRI 0952-0115, along with the $L_{[\text{CII}]} / L_{\text{FIR}}$ observed in the other two high- z sources at higher luminosities, suggest that the [CII] emission is enhanced in high- z galaxies relative to their local counterparts of the same infrared luminosity. Figure 2 shows a linear fit to the high- z [CII]-detected galaxies, in the form

$$\log\left(\frac{L_{[\text{CII}]}}{L_{\text{FIR}}}\right)_{\text{high-}z} = -1.0_{-0.6}^{+0.3} \log(L_{\text{FIR},12}) - 2.3_{-0.3}^{+0.7} \quad (2)$$

(where the errors on the coefficients are dominated by the uncertainty on the magnification factor of BRI 0952-0115, see Appendix). At a given infrared luminosity, the offset between the local and high- z best-fit lines corresponds to an enhancement of the [CII] luminosity by more than an order of magnitude in high- z galaxies. Clearly the result depends on the actual magnification factor of BRI 0952-0115, whose intrinsic L_{FIR} has a

strong leverage on the actual slope of the relation at high redshift. However, even in the case of the highest possible magnification factor ($\mu = 8$, corresponding to the leftmost end of the horizontal red bar in Fig. 2) the evidence of [CII] enhancement, compared to local galaxies of the same infrared luminosity, is still strong.

This result has still low statistical significance, since it is only based on three high- z objects. Moreover, the observed trend may result from selection effects, in the sense that high- z [CII] non-detections may not have been published, so that the three published detections may trace the upper envelope of a wider distribution. Nonetheless, it is worth noting that the three high- z [CII] upper limits available so far (Marsden et al. 2005; Iono et al. 2006, P. Cox priv. comm.)³ are consistent with the high- z [CII]-enhanced scenario, as illustrated in Fig. 2. If the observed effect is confirmed with a larger sample of high- z galaxies, the implied consequences would be quite important, both for the physics of high- z galaxies and for the use of [CII] to search and investigate high- z galaxies in future surveys.

In the following we speculate on the possible origin of the enhanced [CII] emission in high- z galaxies relative to local galaxies of the same luminosity. The offset observed in Fig. 2 between local and high- z galaxies cannot be ascribed to an additional contribution to L_{FIR} because, for instance, of the AGN hosted in these high- z systems (and also present in several of the local galaxies). Indeed, a varying L_{FIR} contribution by AGNs would move objects nearly parallel to the black solid line. Moreover, the far-IR luminosity of (sub-)mm bright quasars (such as the ones discussed here) is generally found to be mostly powered by star formation (Lutz et al. 2007, 2008).

Another possibility is that these high- z galaxies are characterized by lower metallicities of the ISM. Observationally, local low-metallicity galaxies tend to show enhanced [CII] $158 \mu\text{m}$ emission (Rubin et al. 2009; Poglitich et al. 1995; Israel et al. 1996; Madden 2000). The effect is apparent from the location of LMC in Fig. 2 (Rubin et al. 2009). Probably the enhanced [CII] emission in low metallicity galaxies stems from the lower dust content (hence lower dust attenuation to UV photons), which makes the C^+ emitting region larger, and also makes the far-IR emission lower (Rubin et al. 2009). Regardless of the physical origin of the effect, if high- z galaxies are characterized by a reduced metallicity, this may enhance their [CII] emission similarly to local low-metallicity galaxies. High- z star-forming galaxies are indeed observed to have lower gas metallicities than local galaxies (Maiolino et al. 2008). For galaxies hosting quasars, such as the ones investigated here, the situation is more complex. Various studies have found that the metallicity in the broad line region (BLR) of high- z quasars is very high (several times solar) and does not evolve with redshift (Juarez et al. 2009; Jiang et al. 2007; Nagao et al. 2006a). However, the BLR is a very tiny region ($< 1 \text{ pc}$) in quasar nuclei, which is probably not representative of the ISM in the host galaxy, and may undergo quick enrichment with just a few supernova explosions (see detailed discussion in Juarez et al. 2009). A few studies have investigated the metallicity on the larger scales ($\sim 100 \text{ pc} - 10 \text{ kpc}$) of the narrow line region (NLR) in high- z AGNs (Nagao et al. 2006b; Matsuoka et al. 2009; Vernet et al. 2001; De Breuck et al. 2000; Humphrey et al. 2008). These studies are currently limited

to $z < 4$ (i.e. not yet overlapping with our high- z [CII]-sample); however, the inferred NLR metallicities are much lower than in the BLR, about solar or sub-solar, which is indeed less than the metallicity observed in local massive galaxies (Maiolino et al. 2008).

Regardless of the physical origin of the [CII] enhancement in high- z galaxies, if confirmed this effect would have important implications for the planning of future surveys at high- z , as well as for the development of submm/mm facilities. Our result would imply that, at least at high infrared luminosities, the [CII] line in high- z galaxies is about an order of magnitude stronger than previously expected based on local templates. The [CII] line is probably a much more powerful cosmological tool to detect and characterize high- z galaxies than previously thought.

Acknowledgements. We thank the anonymous referee for very helpful comments and M. Bartelmann for useful discussions. We are grateful to the ESO-APEX staff for their support and help during the execution of the project.

References

- Abel, N. P., Dudley, C., Fischer, J., Satyapal, S., & van Hoof, P. A. M. 2009, *ApJ*, in press [arXiv:0903.4643]
- Crawford, M. K., Genzel, R., Townes, C. H., & Watson, D. M. 1985, *ApJ*, 291, 755
- Curran, S. J. 2009, *A&A*, 497, 351
- De Breuck, C., Röttgering, H., Miley, G., van Breugel, W., & Best, P. 2000, *A&A*, 362, 519
- Gerin, M., & Phillips, T. G. 2000, *ApJ*, 537, 644
- Guilloteau, S., Omont, A., Cox, P., McMahon, R. G., & Petitjean, P. 1999, *A&A*, 349, 363
- Humphrey, A., Villar-Martín, M., Vernet, J., et al. 2008, *MNRAS*, 383, 11
- Keeton, C. R. 2001 [arXiv:astro-ph/0102340]
- Iono, D., Yun, M. S., Elvis, M., et al. 2006, *ApJ*, 645, L97
- Israel, F. P., Maloney, P. R., Geis, N., et al. 1996, *ApJ*, 465, 738
- Jiang, L., Fan, X., Vestergaard, M., et al. 2007, *AJ*, 134, 1150
- Juarez, Y., Maiolino, R., Mujica, R., et al. 2009, *A&A*, 494, L25
- Kaufman, M. J., Wolfire, M. G., Hollenbach, D. J., & Luhman, M. L. 1999, *ApJ*, 527, 795
- Lehár, J., Falco, E. E., Kochanek, C. S., et al. 2000, *ApJ*, 536, 584
- Luhman, M. L., Satyapal, S., Fischer, J., et al. 1998, *ApJ*, 504, L11
- Luhman, M. L., Satyapal, S., Fischer, J., Luhman, M. L., et al. 2003, *ApJ*, 594, 758
- Lutz, D., Sturm, E., Tacconi, L. J., et al. 2007, *ApJ*, 661, L25
- Lutz, D., Sturm, E., Tacconi, L. J., et al. 2008, *ApJ*, 684, 853
- Madden, S. C. 2000, *New Astron. Rev.*, 44, 249
- Maiolino, R. 2008, *New Astron. Rev.*, 52, 339
- Maiolino, R., Maiolino, R., Cox, P., Caselli, P., et al. 2005, *A&A*, 440, L51
- Maiolino, R., Nagao, T., Grazian, A., et al. 2008, *A&A*, 488, 463
- Malhotra, S., Kaufman, M. J., Hollenbach, D., et al. 2001, *ApJ*, 561, 766
- Marsden, G., Borys, C., Chapman, S. C., et al. 2005, *MNRAS*, 359, 43
- Matsuoka, K., Nagao, T., Maiolino, R., Marconi, A., & Taniguchi, Y. 2009, *A&A*, submitted
- Nagao, T., Marconi, A., & Maiolino, R. 2006a, *A&A*, 447, 157
- Nagao, T., Maiolino, R., & Marconi, A. 2006b, *A&A*, 447, 863
- Negishi, T., Onaka, T., Chan, K.-W., & Roellig, T. L. 2001, *A&A*, 375, 566
- Poglitich, A., Krabbe, A., Madden, S. C., et al. 1995, *ApJ*, 454, 293
- Priddey, R. S., & McMahon, R. G. 2001, *MNRAS*, 324, L17
- Rubin, D., Hony, S., Madden, S. C., et al. 2009, *A&A*, 494, 647
- Rusin, D., Kochanek, C. S., & Keeton, C. R. 2003, *ApJ*, 595, 29
- Sanders, D. B., & Mirabel, I. F. 1996, *ARA&A*, 34, 749
- Spergel, D. N., Verde, L., Peiris, H. V., et al. 2003, *ApJS*, 148, 175
- Stacey, G. J., Geis, N., Genzel, R., et al. 1991, *ApJ*, 373, 423
- Treu, T., & Koopmans, L. V. E. 2004, *ApJ*, 611, 739
- Vassilev, V., Meledin, D., Lapkin, I., et al. 2008, *A&A*, 490, 1157
- Vernet, J., Fosbury, R. A. E., Villar-Martín, M., et al. 2001, *A&A*, 366, 7
- Walter, F., Riechers, D., Cox, P., et al. 2009, *Nature*, 457, 699
- WeiB, A., Downes, D., Neri, R., et al. 2007, *A&A*, 467, 955
- Wright, E. L., Mather, J. C., Bennett, C. L., et al. 1991, *ApJ*, 381, 200

³ BR 1202-0725 was included in Maiolino et al. (2005) as an upper limit (from Benford et al., in prep.), but subsequently Iono et al. (2006) detected [CII] in the northern component of the source, while the southern component remained undetected. Both components are consistent with the high- z relation shown in Fig. 2.

Appendix A: The lensing magnification factor

Although $L_{[\text{CII}]} / L_{\text{CO}}$ and $L_{[\text{CII}]} / L_{\text{FIR}}$ most likely do not depend on the magnification factor, since [CII], CO, and FIR are emitted from the same regions of the galactic gaseous disk, the inferred intrinsic luminosities, and in particular L_{FIR} , do depend on the magnification factor. Therefore, especially for what concerns the $L_{[\text{CII}]} / L_{\text{FIR}}$ versus L_{FIR} diagram, it is important to address the issue of the magnification lensing factor in detail.

Guilloteau et al. (1999) provided only a rough estimate of the magnification factor ($\mu \sim 4$). Lehar et al. (2000) performed a more detailed lensing analysis by using different mass models for the lensing galaxy along with HST images (although they do not directly provide the associated magnification factors). The positions and the flux ratio of the two quasar images are reproduced by a singular-isothermal-ellipsoid model (SIE). A constant M/L model, where the lensing mass distribution matches the light distribution of the observed galaxy, plus an external shear γ (due to galaxies surrounding the lens) also provides a good fit to the data. Details on the best-fit parameters describing the lensing models can be found in Table 5 of Lehar et al. (2000). Based on the image constraints, it is impossible to differentiate between the SIE and the M/L models. We used the public software *GRAVLENS* and its application *LENMODEL* (Keeton 2001) to repeat the fits by Lehar et al. (2000) and to reconstruct their lens models. These were used to estimate the magnification factors at the positions of the two quasar images. The lens is a typical early-type galaxy, whose light distribution can be described by means of a De Vaucouleurs profile. The two models predict significantly different magnification factors. Assuming a point source, the SIE and the $M/L + \gamma$ models give total magnification factors $\mu = 8$ and $\mu = 2.5$, respectively. The large difference is caused by the substantially different slopes of the two density profiles, with the SIE much steeper than the De Vaucouleurs profile. Without an external shear, the SIE model may be overestimating the lens convergence and therefore the magnification. However, since no correlation is expected between the external shear and the environment of the lens galaxy, it is hard to estimate the possible bias (see the discussion in Lehar et al. 2000). In the $M/L + \gamma$ model, even a modest external shear strongly perturbs the lens. In general, steeper profiles

are favored by observations of strong lensing systems (e.g. Rusin et al. 2003; Treu & Koopmans 2004). Therefore we can assume that the magnification factor predicted by the $M/L + \gamma$ model is a lower limit to the true value.

By using the result of the fit of the quasar double image, we attempted to estimate how much the magnification factor changes for an extended source. This is important in our case since the [CII] and the FIR emissions come from an extended region of the gaseous disk of the quasar host galaxy. For instance, in the case of J1148+5251 at $z = 6.41$, high angular resolution images show that [CII] is distributed in a region of about 1.5 kpc in diameter around the quasar (Walter et al. 2009). By replacing, on the source plane, the point-like source (the quasar nucleus observed in the optical images) with a circular disk (the [CII]-FIR emitting region) of radius $0.2''$ (equivalent to $\sim 1 \text{ h}^{-1} \text{ kpc}$ at $z = 4.43$) centered on the location of the un-lensed quasar (from the modeling of its point images), and mapping it on the lens plane, we find that the total magnification factors change by $\lesssim 0.5$ for both the SIE and the $M/L + \gamma$ models. The magnification factor does not change significantly when varying the size of the [CII]-FIR disk as long as it is less than 2 kpc in radius. However, we note that the morphology of the extended images is very different for the two models. In particular, the SIE model produces an Einstein ring-like image, while the $M/L + \gamma$ model produces an extended asymmetric arc and a counter image. Therefore, high angular resolution observations of the [CII] and FIR emission would allow us to determine which of the two lens models is more appropriate.

In summary, the magnification factor ranges between $\mu = 2.5$ and $\mu = 8$, mostly depending on the lens model. In the paper we assume a magnification factor $\mu = 4.5$ (the mean value of the two extreme magnification factors in log) as a reference, although we discuss the implications of the wide range of possible magnification factors. For what concerns the intrinsic far infrared luminosity, the observed value $L_{\text{FIR}} = 1.7 \times 10^{13} L_{\odot}$ inferred by Priddey & McMahon (2001) (and corrected for our assumed cosmology) translates into an intrinsic, magnification-corrected, far-infrared luminosity of $L_{\text{FIR}} = 4_{-2}^{+3} \times 10^{12} L_{\odot}$, where the errors reflect the range in possible magnification factors.